Reactivity of Mixed phosphonodithioato-dppt Ni^{II} mixed complexes with halogens: First Example of a Metal-Coordinating Tribromide Anion

M. Carla Aragoni, Massimiliano Arca, Francesco A. Devillanova, Michael B. Hursthouse, Susanne L. Coles Huth, Francesco Isaia and Vito Lippolis

SUPPORTING INFORMATION

Table of Contents:

CRYSTAL STRUCTURE METHODS, DATA, AND DISCUSSION

X-ray Diffraction: Crystallographic data were collected at 120(2) K for all compounds by means of combined phi and omega scans on a Bruker-Nonius FR591 area detector, situated at the window of a rotating anode (graphite Mo-K_α radiation and 10cm confocal mirrors, $\lambda = 0.71073$Å). The structures were solved by direct methods, SHELXS-97 and refined on F^2 using SHELXL-97.[S1] Anisotropic displacement parameters were assigned to all non-hydrogen atoms. Hydrogen atoms were included in the refinement, but thermal parameters and geometry were constrained to ride on the atom to which they are bonded. The data were corrected for absorption effects using SADABS 2007/2 for **1**,[S2] and SADABS V2.10 for $[Ni(MeOpdt)_2\cdot(dppt)_2]$(**1**$^{(S)}$) and **2**.[S3] The structure of **1** was refined as a racemic twin, and the absolute configuration cannot be determined reliably. There are solvent accessible voids in the structure of **1** and **2**, but no solvent could be located within these.

The details of the crystal structure investigation have been deposited at the Cambridge Crystallographic Data Centre as supplementary publications no. XXXX. Copies of the data can be obtained free of charge on application to CCDC, 12 Union Road, Cambridge CB2 1EZ, UK [fax: int. code + 44(1223)336-033, e-mail: deposit@ccdc.cam.ac.uk].

Description of the Crystal Structures: The preparation of the precursor complex *trans*-$[Ni(MeOpdt)_2\cdot(dppt)_2]$ [**1**$^{(S)}$; dppt: bis(5,6-diphenyl-3-(2-pyridyl)-1,2,4-triazine); MeOpdt = $(4\text{-}CH_3\text{-}OC_6H_5)(CH_3O)PS_2^-$, i.e. *O*-methyl-4-methoxyphenyl-phosphonodithioate, Figure S1, Tables S1 and S2] follows our recent studies on the reactivity of coordinatively unsaturated phosphonodithioato Ni^{II} complexes[S4] with monodentate donor molecules,[S5] bidentate bipyridyl-based spacers,[S6] and *multi-modal* ligands.[S7] The reaction of the phosphonodithioate complex *trans*-$[Ni(MeOpdt)_2]$ with dppt engenders an expansion and rearrangement of the nickel coordination sphere from square planar to octahedral. The Ni^{II} ion lies on an inversion centre and the asymmetric unit consists of a half of the complex molecule. The metal ion is coordinated in the equatorial plane by two pyridine (N4) and two triazine (N2) nitrogens; the apical positions are occupied by two sulphur atoms (S1) belonging to two phosphonodithioates forced to behave as monodentate ligands. The formation of five-membered chelate rings with small rigid N–Ni–N bites [N1–Ni–N4 78.67(7)°] is reflected in the geometry around the nickel, with N-Ni-S angles diverging from the ideal values of 90° (Table 2). The Ni–S bond length falls in the range expected for phosphonodithioato fragments belonging to octahedral complexes; the two Ni–N1/N4 bond distances are only slightly different and comparable with those found in similar nickel complexes containing pyridine based ligands.[S8] The triazine and pyridine rings that define the equatorial coordination plane are roughly planar being angled at 7.9° (N1–C11–C28–N4 5.06°); the two phenyl rings bound to the triazine ring are twisted by 37.4° and 138.7° with respect to the triazine plane in order to maximize intramolecular and intermolecular interactions [Figures S2 and S3].

When reacted with Br_2 and I_2 the complex **1**$^{(S)}$ underwent complete substitution of the phosphonodithioato ligands from the Ni^{II} coordination sphere, leading to *cis*-$[Ni(dppt)_2(Br_3)_2]$ (**1**) and *trans*-$[Ni(dppt)_2(I)_2]$ (**2**), respectively. The reaction with elemental bromine yielded complex *cis*-$[Ni(dppt)_2(Br_3)_2]$ (**1**), shown in Figure 1, for which crystal and structural data are reported in Tables S1 and S2, respectively. The crystal structure of complex **1** is described in the communication. The crystal packing is built up by interactions between the tribromide anions and the phenyl hydrogen atoms of neighboring molecules (Figure S4). The symmetry related interacting molecules present different orientations, thus generating the packing showed in Figure S5. Single crystal X-ray diffraction analysis of **2** reveals that the neutral complex *trans*-$[Ni(dppt)_2(I)_2]$ presents a coordination environment similar to that of $\mathbf{1}^{\mathbf{(S)}}$ with two iodides in place of the two phosphonodithioato monodentate ligands MeOpdt originally present. Crystal data and selected bond lengths and angles for **2** are reported in Tables S1 and S2; Figure 2 (bottom) shows the complex unit, along with the atom labeling scheme. Nickel–nitrogen bond distances and angles are comparable to those found for complex $\mathbf{1}^{\mathbf{(S)}}$; the Ni–I distance [2.7707(3) Å] falls within the range found for octahedral nickel complexes containing an iodide ligand.[S9] Similarly to what is observed in $\mathbf{1}^{\mathbf{(S)}}$, the triazine and pyridine rings are roughly planar, with an angle of 6.1° between the rings (N1–C3–C16–N4 3.25°). The two phenyl rings are angled at 28.1 and 45.4° with respect to the triazine ring, thus favoring mutual edge-to-edge interactions involving adjacent molecules which govern the resulting packing (Figure S6).

THEORETICAL CALCULATIONS

Experimental. Quantum-chemical DFT calculations were carried out on complex $\mathbf{1}^{\mathbf{(S)}}$ and on compounds **1**–**8** with the mPW1PW[S10] hybrid functional and Schäfer, Horn, and Ahlrichs double-zeta plus polarization all-electron basis sets (BSs)[S11] using the commercially available suite of programs Gaussian09.[S12] Calculations were performed on the involved compounds both in their triplet and single ground states, the former resulting energetically more stable and with electronic and structural features better meeting the experimental data. All optimized geometries were verified by a vibrational analysis. NBO charge distributions[S13] and Wiberg bond indexes[S14] were calculated at the optimized geometries.[S15] The programs Gabedit 2.0.7[S16] and Molden 5.0[S17] were used to investigate the charge distributions and molecular orbital shapes. The atomic coordinates in orthogonal Cartesian format as well as the log files can be obtained from the authors by request.

Electronic Structures and Frontier Molecular Orbitals. The Kohn-Sham HOMO of $\mathbf{1}^{\mathbf{(S)}}$ is mainly due to a symmetric combination of non bonding p-orbitals of the sulfur atoms of the phosphonodithioato ligands, whilst the HOMO of compound **2** mainly involves the antibonding combination of the axial iodides p_z orbitals with the d_{z^2} AO of the nickel ion, with only minor contributions from the nitrogen atoms of the dppt ligands (Figures S8a and S8c). In both compounds $\mathbf{1}^{\mathbf{(S)}}$ and **2,** KS–LUMO's are combinations of π antibonding orbitals mainly localized on the triazine rings (Figures S8b and S8d). The frontier orbitals calculated for compound **8**, featuring bromide ligands axially bound to the nickel ion, are similar in nature to those described for **2** (Figures S9e and S9f). When monohalides are bound to the nickel ion in a *cis*-configuration (**6** and **7**) the HOMO's are recognizable as non-bonding p orbitals of the coordinated halides

(Figures S9a and S9c), whilst the LUMO are mainly centred on the triazine rings of the dppt ligands, similarly to those calculated for the *trans* analogues (Figures S9b and S9d).

NBO Analysis. In $\mathbf{1^{(S)}}$, as expected, the uncoordinated sulphur atom (S2, -0.672 e) is more negatively charged than that coordinating the nickel centre (S1, -0.554 e). An examination of the charge distribution on the dppt ligands in $\mathbf{1^{(S)}}$ shows that the nitrogen donor atom N1 belonging to the triazine ring is less negatively charged than N4, belonging to the coordinating pyridine ring (N1, -0.279; N2, -0.198; N4, -0.487 e). Since the NBO analysis clearly indicates second order contributions from the N1─N2 bonding natural orbital to the empty Ni 3d AO's, the ensemble N1─N2 can be considered as far as the charge distribution is regarded. Indeed, the negative charge calculated for N4 is comparable with the sum of those on N1 and the adjacent N2. This explains the very small differences between the two Ni–N bond distances, also reflected in the very similar Wiberg bond index (WBIs) calculated between the metal and the nitrogen atoms (Ni─N1, 0.258; Ni─N4, 0.254).

Second Order Perturbation of the Fock Matrix. The analysis of the interaction of the N1 (N4) lone pairs with the 3*d* AO's localised on the nickel ion showed very similar values for all the examined compounds: $\mathbf{1^{(S)}}$, 38.8 (35.7); **1**, 42.2 (36.5); **2**, 39.1 (38.3); **3**, 41.6 (39.7); **4**, 41.1 (40.7); **5**, 40.2 (38.1); **6**, 38.9 (40.4); **7**, 40.9 (42.3); **8**, 40.3 (39.3 kcal mol^{-1}). As regards the coordinating halides or trihalides, the interactions between the lone pairs localized on the halogen atoms directly bound to the metal and the empty *d*-NBOs on the nickel centre were calculated to be 70.2, 104.2, 76.6, 83.9, 82.8, 105.2, 99.8, 98.7 kcal mol^{-1} for **1-8**, respectively.

EXPERIMENTAL SECTION

Materials and Methods. All the reagents and solvents were purchased from Aldrich or Lancaster, and used without further purification. Elemental analyses were performed with an EA1108 CHNS-O Fisons instrument. FT-Infrared spectra were recorded on a Thermo Nicolet 5700 spectrometer at room temperature. Middle IR spectra (resolution 4 cm^{-1}) were recorded as KBr pellets, with a KBr beam-splitter and KBr windows.

Syntheses. *Trans*-bis[*O*-methyl-(4-methoxyphenyl)dithiophosphonato]Ni complex [Ni(MeOdtp)$_2$] was synthesized according to previously reported procedures.[S5]

[Ni(MeOpdt)$_2$·(dppt)$_2$] ($\mathbf{1^{(S)}}$): dppt (63.0 mg; 0.20 mmol) and [Ni(MeOdtp)$_2$] (52.8 mg; 0.10 mmol) were heated in 30 mL of MeOH in an Ace pressure tube until complete dissolution. The product was obtained as dark red crystals by slow evaporation of the solution at room temperature. Mp 130°C. Elemental analysis found (calc. for $C_{56}H_{48}N_8NiO_4P_2S_4$): C, 58.84 (58.70); H, 4.28 (4.22); N, 9.32 (9.38); S, 11.02 (11.19). Yield: 82.3 mg, 0.0718 mmol, 72%. FT-IR (1700–400 cm^{-1}): 1594 s, 1559 m, 1541 m, 1517 vs, 1497 vs, 1446 ms, 1406 vs, 1373 vs, 1290 m, 1249 s, 1177 m, 1111 ms, 1024 vs, 829 w, 798 m, 770 s, 697 s, 667 s, 624 m, 603 m, 543 ms, 420 w cm^{-1}.

[Ni(dppt)$_2$(Br$_3$)]$_2$ (1). **1**$^{(S)}$ (8.3 mg; 0.0072 mmol) and 0.45 mL of a CH_2Cl_2 solution of Br_2 0.011 M (0.0050 mmol) were reacted in CH_2Cl_2. The product was obtained as dark-saffron crystals by slow evaporation of the solution at room temperature (Yield: 4.0 mg, 0.0034 mmol, 69%). Elemental Anal. Found (Calc.) for $C_{40}H_{28}Br_6N_8Ni_2$: C, 41.41 (41.46); H, 2.40 (2.44); N, 9.64 (9.67); FT-IR (1700–500 cm^{-1}): 1606m, 1518vs, 1481s, 1446s, 1408vs, 1374vs, 1319w, 1287w, 1259mw, 1180w, 1150mw, 1137mw, 1101w, 1074w, 1048w, 1040w, 1024w, 1014mw, 922w, 885w, 846w, 826w, 794w, 770s, 760ms, 750w, 733w, 696vs, 675mw, 648w, 604m, 539mw, 515w cm^{-1}.

[Ni(dppt)$_2$(I)$_2$] (2). **1**$^{(S)}$ (58.0 mg; 0.051 mmol) and I_2 (25.5 mg; 0.10 mmol) were reacted in 30 mL of a MeOH/$CHCl_3$ 1:1 mixture. The product was obtained as deep orange crystals by slow evaporation of the solution at room temperature (Yield: 26.0 mg, 0.028 mmol, 56%). Elemental Anal. Found (Calc.) for $C_{40}H_{28}I_2N_8Ni$: C, 51.39 (51.48); H, 2.97 (3.02); N, 11.80 (12.01); FT-IR FT-IR (1700–500 cm^{-1}): 1597s, 1577m, 1514vs, 1481vs, 1445s, 1406vs, 1371vs, 1317m, 1304m 1289m, 1257ms, 1180w, 1156mw, 1129mw, 1098w, 1074w, 1050w, 1038w, 1012ms, 921w, 883w, 844w, 791w, 767s, 757s, 744mw, 709w, 693vs, 677ms, 647mw, 603mw, 535mw, 513w cm^{-1}.

FIGURES

Figure S1: Molecular view of **1$^{(S)}$**. For clarity hydrogen atoms have been omitted. Displacement ellipsoids are drawn at 50% probability level. Symmetry code: ' 1-x, 1-y, 1-z.

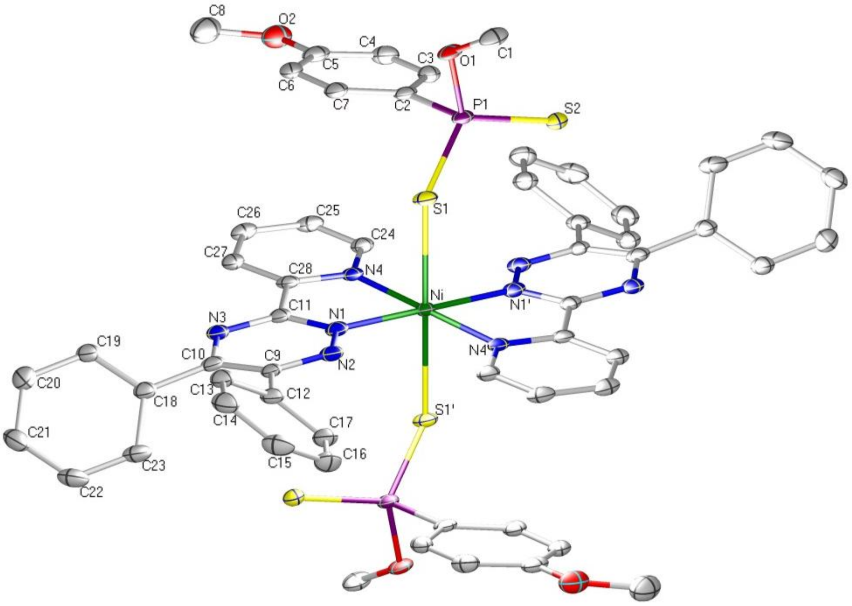

Figure S2: Packing view of **1$^{(S)}$** evidencing the ribbons, running in the *a* direction, built up through H-bonds involving the oxygen atoms of the methoxy P-substituents and the phenyl rings bound to the triazine. H-atoms not involved in showed interactions have been omitted for clarity. Symmetry code: ' -1+x, y, z.

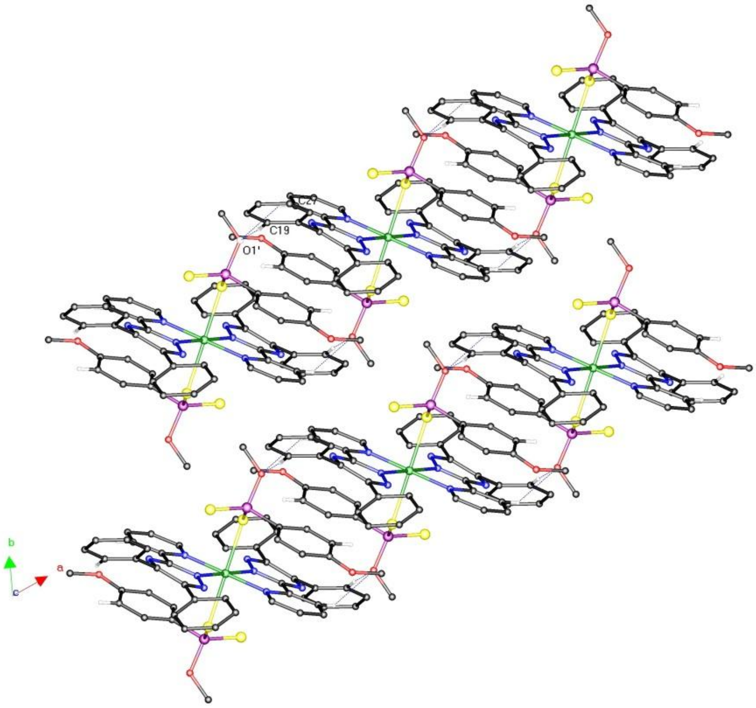

Figure S3: View of $\mathbf{1}^{(S)}$ evidencing the packing of the ribbons along the *c* direction. Hydrogen atoms have been omitted for clarity.

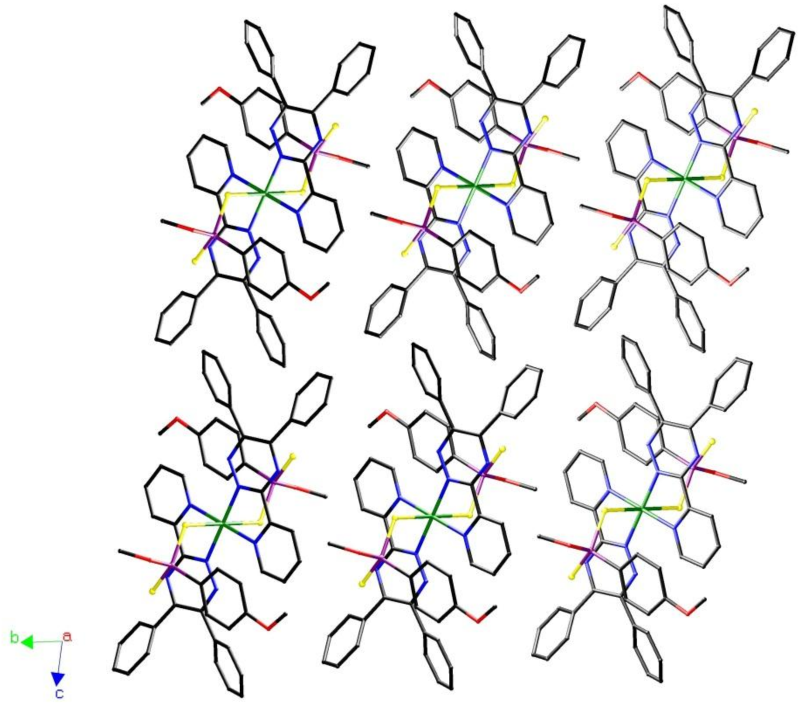

Figure S4: View of the packing of complex **1** built up through Br···H interactions among adjacent molecules: Br3···H18', 2.987; Br3···H19', 2.950; Br3···H13'', 2.892; Br2···H7''', 2.970 Å. H-atoms not involved in showed interactions have been omitted for clarity. Symmetry codes: ' 0.5-x, -0.5+y, 0.5-z; '' 2-y, x, -z; ''' 1.5-x, -0.5+y, 0.5-z.

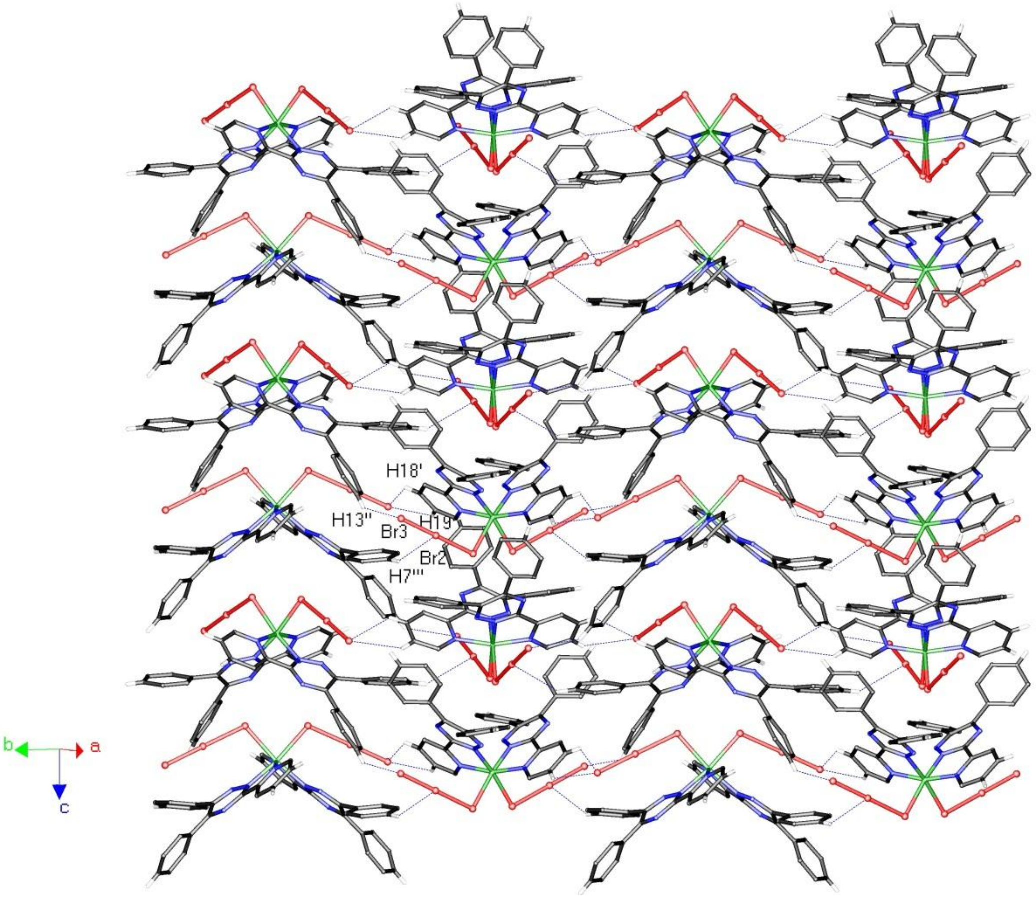

Figure S5: Packing view of **1** along the *c* axis showing the voids within the crystal structures evidenced in blue color. The voids (100.7 Å^3, 2.4% of the unit cell volume) within the crystal structure have been calculated based on contact surface by using Mercury 2.4, with a probe radius of 1.2 Å and a grid space of 0.5 Å. Hydrogen atoms have been omitted for clarity reasons.

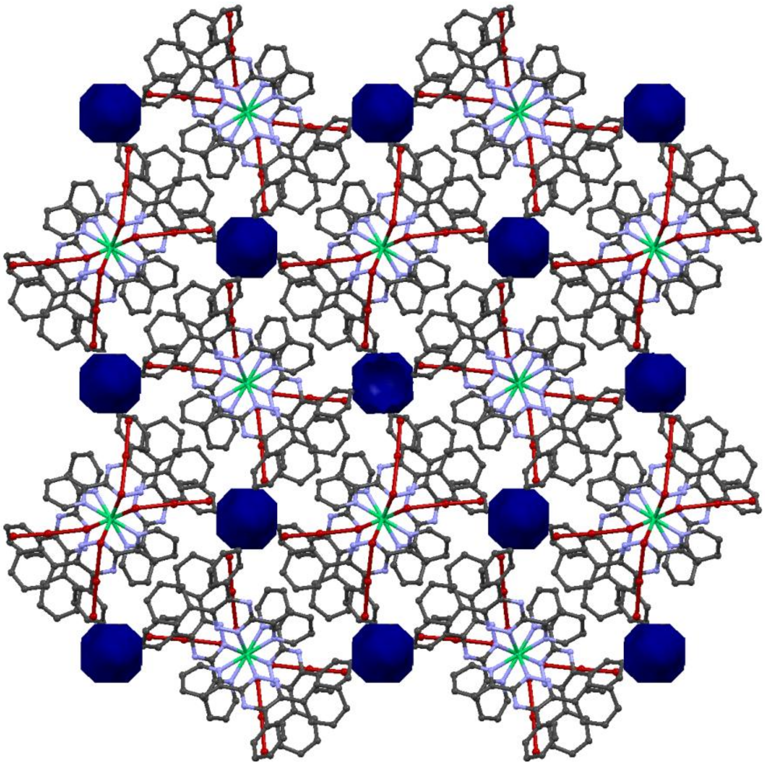

Figure S6: Packing view of **2** showing the complex molecules interacting trough H···I contacts involving the coordinated iodides and the phenyl rings bound to the triazine. The phenyl rings protruded beyond the ribbons edge-to-edge interact (H14····Cnt$_{[C4\text{-}C9]}$ = 3.96 Å) along the *a* direction, defining the packing.

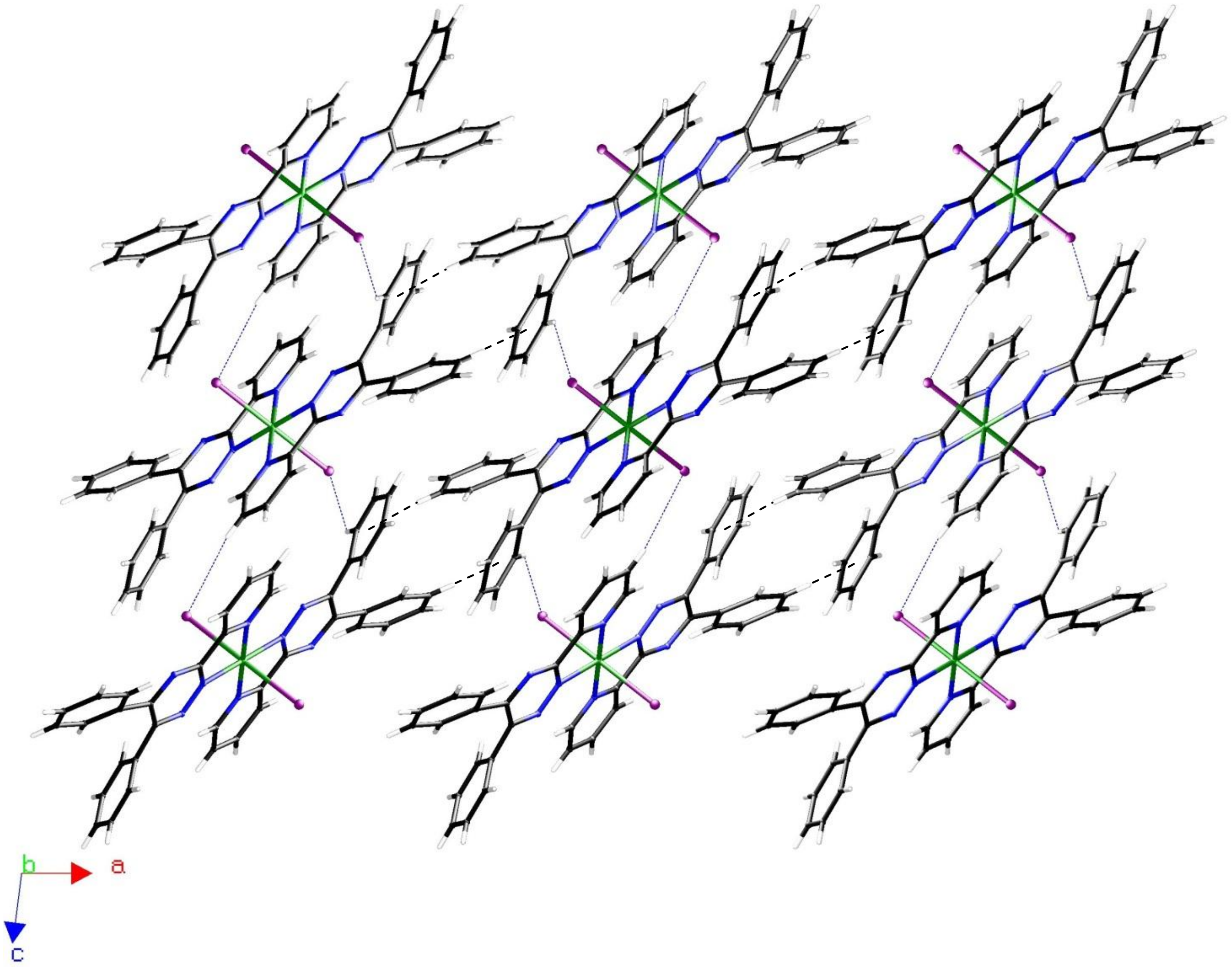

Figure S7: Scatter plot of Br1─Br2 *versus* Br2─Br3 distances for linear tribromides from a search on CSD. The points refer to 142 fragments featuring Br1─Br2─Br3 angles > 170° from 107 different structures with R<0.1; CSD (v. 5.33, 2012); empty dot: **1**

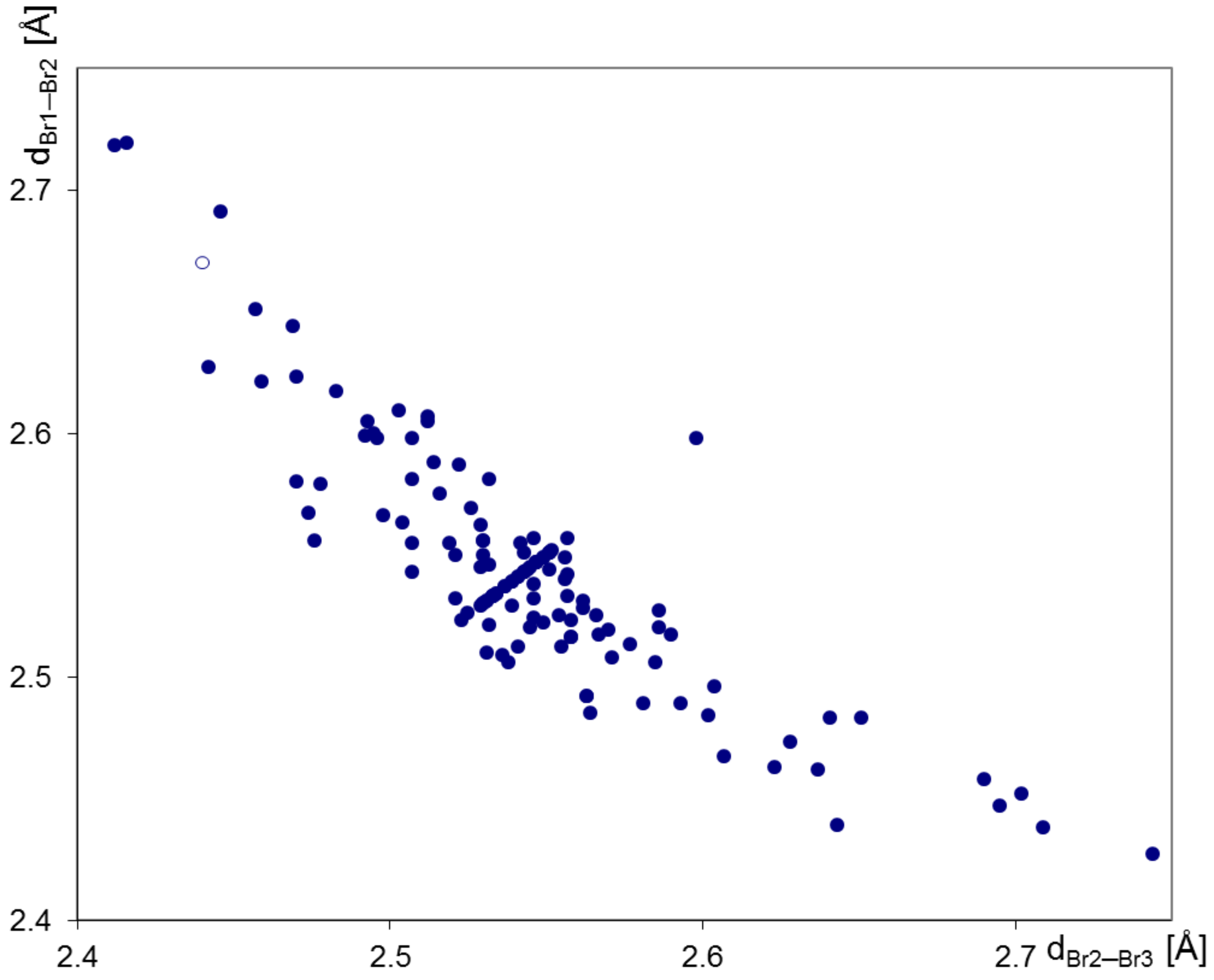

Figure S8: Drawings of the calculated Kohn-Sham alpha frontier molecular orbitals of complex **1**$^{(S)}$ (a, HOMO; b, LUMO), and **2** (c, HOMO; d, LUMO). Contour value = 0.05 e.

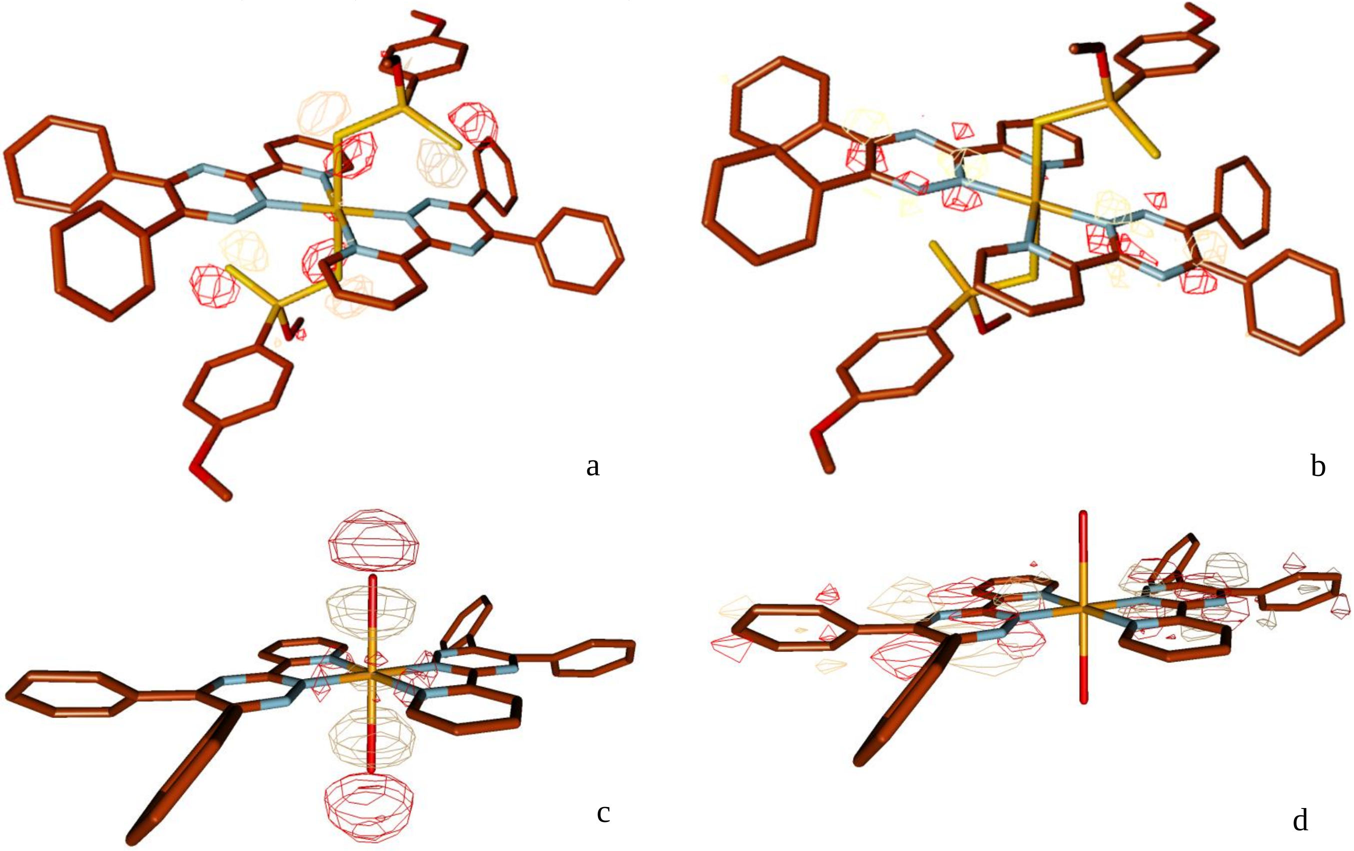

Figure S9: Drawings of the Kohn-Sham alpha frontier molecular orbitals of complex **6** (a, HOMO; b, LUMO), **7** (c, HOMO; d, LUMO), and **8** (e, HOMO; f, LUMO). Contour value = 0.05 e.

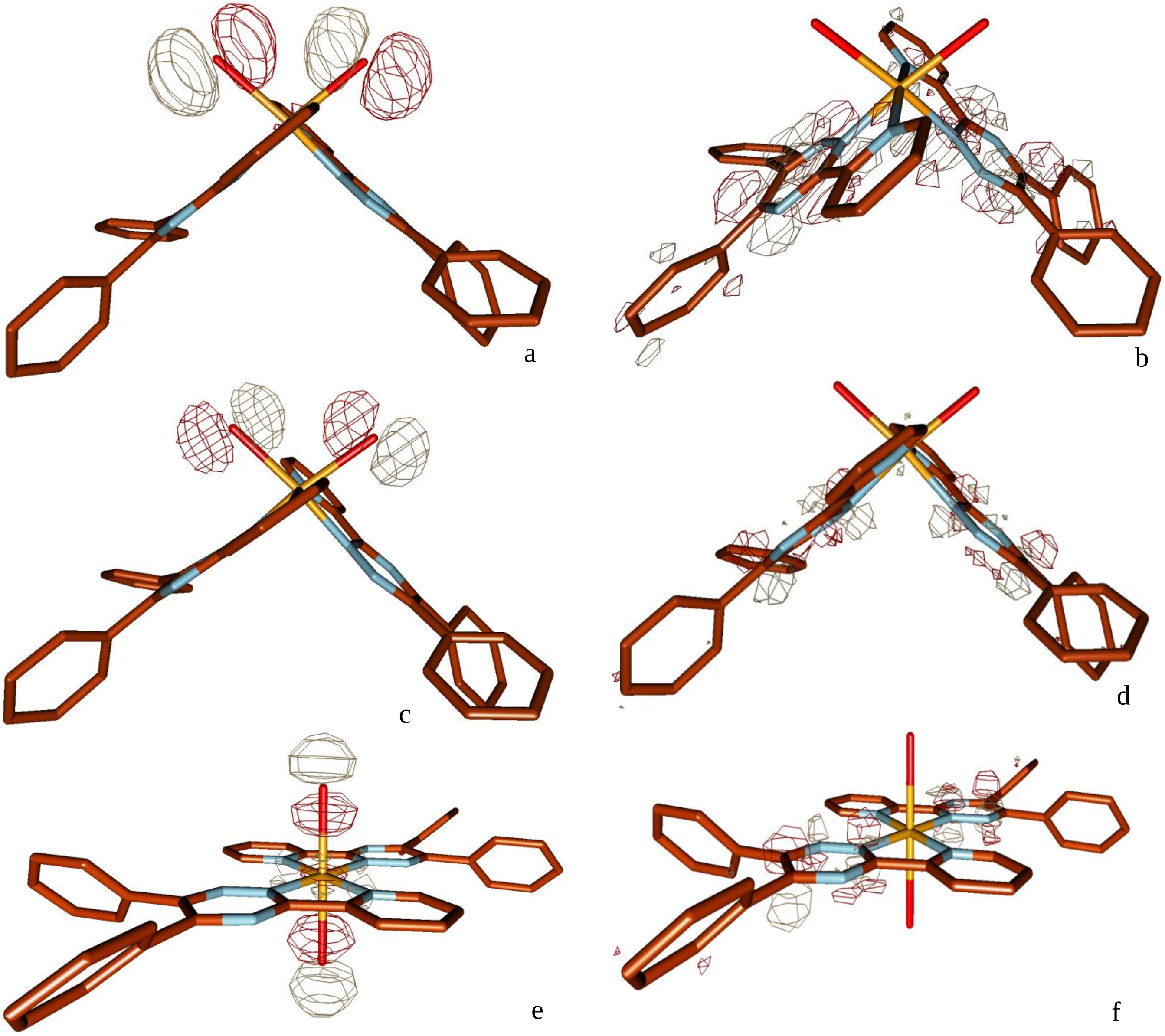

TABLES

Table S1. Crystal data collections and refinements for compounds **1**$^{(S)}$, **1** and **2**

	1$^{(S)}$	**1**	**2**
Empirical formula	$C_{56}H_{48}N_8NiO_4P_2S_4$	$C_{40}H_{28}Br_6N_8Ni$	$C_{40}H_{28}I_2N_8Ni$
M	1145.93	1158.79	933.19
Crystal system	Triclinic	Tetragonal	Monoclinic
Space group	*P-1* (no. 2)	*P*-421c (no. 114)	*C2/c* (no. 15)
a (Å)	9.2767(11)	17.3688(1)	25.0178(10)
b (Å)	10.467(2)	17.3688(1)	8.8338(2)
c (Å)	15.0969(13)	13.8272(2)	16.5583(6)
α (°)	79.283(13)	90	90
β (°)	84.701(8)	90	97.264(2)
γ (°)	65.476(16)	90	90
Volume (Å^3)	1310.2(4)	4171.32(7)	3630.1(2)
Z	1	4	4
D_{calc} (Mg/m^3)	1.452	1.845	1.707
μ (mm^{-1})	0.647	6.253	2.277
θ min-max (°)	3.0-27.5	3.2-27.5	3.1-27.5
Refl.Collected/unique	26207/5955	76045/4788	20594/4173
Refl.obs.(I>2σI)	4790	4001	3603
R/R_{INT}	0.0416/0.059	0.0514/0.095	0.0416/0.046
wR2	0.0991	0.1146	0.1101

Table S2. Selected bond lengths (Å) and angles (°) for compounds $\mathbf{1}^{(S)}$, **1** and **2**.

	$\mathbf{1}^{(S)}$	**1**	**2**
Ni–N1	2.0823(19)	2.044(5)	2.063(4)
Ni–N4	2.1021(19)	2.064(5)	2.102(3)
Ni–S1	2.5059(8)		
Ni–S2			
P1–S1	2.0189(9)		
P1–S2	1.9717(10)		
Ni–I1/Br1		2.5772(12)	2.7707(3)
Br1–Br2		2.6760(12)	
Br2–Br3		2.4406(14)	
S1-Ni-N1	85.10(6)		
S1-Ni-N4	91.80(6)		
S1-Ni-N1'	94.90(6)		
S1-Ni-N4'	88.20(6)		
N1-Ni-N4	78.67(7)	78.9(2)	78.59(13)
N1-Ni-N4'	101.33(7)	90.5(2)	101.41(13)
N1–Ni–N1'	180.00	98.9(2)	180.00
N4–Ni–N4'	180.00	163.7(2)	180.00
S1–P–S2	118.06(5)		
I1/Br1–Ni–N1		172.23(16)	89.94(10)
I1/Br1–Ni–N4		100.91(15)	87.89(9)
I1/Br1–Ni–N1'		88.84(15)	90.06(10)
I1/Br1–Ni–N4'		91.29(15)	92.11(9)
I1/Br1–Ni–I1'/Br1'		83.40(4)	180.00
Br2–Br1–Ni		106.83(4)	
Br1–Br2–Br3		178.07(4)	

Table S3. Total electronic energy E_0 (Hartree), Zero-Point energy corrections ZPE (Hartree), and energy difference $\Delta E_{cis\text{-}trans}$ (Hartree, kcal mol^{-1} in parentheses) between the *cis* and *trans* isomers for compounds **1**–**8** of general formula [Ni(dppt)L_2], I_2 and Br_2 calculated at DFT level.[a]

L	Br_3^-	Br_3^-	I_3^-	I_3^-	Br^-	Br^-	I^-	I^-		
Isomer	*cis*	*trans*	*cis*	*trans*	*cis*	*trans*	*cis*	*trans*		
Compound	**1**	**3**	**4**	**5**	**7**	**8**	**6**	**2**	I_2	Br_2
E_0	-2225.827014	-2225.826737	-2215.196311	-2215.198626	-2173.095525	-2173.101038	-2169.534445	-2169.54434	-22.79705	-26.79705
ZPE	0.605968	0.606249	0.604883	0.605446	0.602533	0.603165	0.602143	0.603097	0.000434	0.000644
E_0+ZPE	-2225.221046	-2225.220488	-2214.591428	-2214.593180	-2172.492992	-2172.497873	-2168.932302	-2168.941243	-22.79662	-26.33019
$\Delta E_{cis\text{-}trans}$	–	-0.000558	–	0.001753	–	0.004881	–	0.008941	–	–
		(-0.350)		(1.100)		(3.063)		(5.610)		

[a] mPW1PW functional; Shafer, Horn, and Ahlrichs pVDZ basis set.

REFERENCES

[S1] G. M. Sheldrick, SHELX suite of programs for crystal structure solution and refinement, Univ. of Göttingen, Germany, 1997.
[S2] Sheldrick, G. M. SADABS 2007/2.
[S3] Sheldrick, G. M. SADABS V2.10, 2003.
[S4] M. Arca, A. Cornia, F. A. Devillanova, A. C. Fabretti, F. Isaia, V. Lippolis, and G. Verani *Inorg. Chim. Acta* (1997), **262** (**1**), 81-84. I. Haiduc, "1,1-Dithiolato ligands and related selenium and tellurium compounds", in *Handbook of Chalcogen Chemistry, New Perspectives in Sulfur, Selenium and Tellurium*, F. A. Devillanova, Ed., chapter 10.2 (pp. 593-643), Royal Society of Chemistry, London, UK, 2006.
[S5] M. C. Aragoni, M. Arca, F. Demartin, F. A. Devillanova, C. Graiff, F. Isaia, V. Lippolis, A. Tiripicchio, and G. Verani *J. Chem. Soc., Dalton Trans.* (2001) 2671-2677.
[S6] M. C. Aragoni, M. Arca, N. R. Champness, A. V. Chernikov, F. A. Devillanova, F. Isaia, V. Lippolis, N. S. Oxtoby, G. Verani, S. Z. Vatsadze, and C. Wilson *Eur. J. Inorg. Chem.* (2004), **10**, 2008-2012. M. C. Aragoni, M. Arca, N. R. Champness, M. De Pasquale, F. A. Devillanova, F. Isaia, V. Lippolis, N. S. Oxtoby, G. Verani, and C. Wilson *CrystEngComm* (2005), **7**(**60**), 363-369. M. C. Aragoni, M. Arca, M. Crespo, F. A. Devillanova, M. B. Hursthouse, S. L. Huth, F. Isaia, V. Lippolis, and G. Verani *CrystEngComm* (2007), **9** (**10**), 873-878.
[S7] M. C. Aragoni, M. Arca, F. A. Devillanova, M. B. Hursthouse, S. L. Huth, F. Isaia, V. Lippolis, A. Mancini, S. Soddu, and G. Verani *Dalton Trans.* (2007), **21**, 2127-2134. M. C. Aragoni, M. Arca, M. Crespo, F. A. Devillanova, M. B. Hursthouse, S. L. Huth, F. Isaia, V. Lippolis, and G. Verani *Dalton Trans.* (2009), **14**, 2510-2520.
[S8] Due to the lack of similar complexes: no other dppt nickel complexes have been structurally characterised so far, a search in the Cambridge Database CSD (v. 5.32, May 2011 updated) has been performed on octahedral nickel complexes containing at least one piridyl ligand, finding a Ni–N mean value of 2.089 Å (calculated on 3083 structures, 9414 fragments).
[S9] A search in the CSD (v. 5.32, May 2011 updated) made on the nickel complexes containing an iodide ligand (144 structures, 214 fragments) showed that the Ni–I bond distances mainly depend on the coordination geometry around the nickel(II) ion; for octahedral complexes (25 structures, 33 fragments, $R < 0.1$) we found Ni–I bond distances ranging between 2.694 and 2.887 Å and a mean value of 2.789 Å.
[S10] C. Adamo and V. Barone, *J. Chem. Phys*. (1998**)**, **108**, 664.
[S11] Schafer, A.; Horn H.; Ahlrichs, R. *J. Chem. Phys.* **1992,** *97*, 2571.
[S12] Gaussian 09, Revision A02, M. J. Frisch, G. W. Trucks, H. B. Schlegel, G. E. Scuseria, M. A. Robb, J. R. Cheeseman, G. Scalmani, V. Barone, B. Mennucci, G. A. Petersson, H. Nakatsuji, M. Caricato, X. Li, H. P. Hratchian, A. F. Izmaylov, J. Bloino, G. Zheng, J. L. Sonnenberg, M. Hada, M. Ehara, K. Toyota, R. Fukuda, J. Hasegawa, M. Ishida, T. Nakajima, Y. Honda, O. Kitao, H. Nakai, T. Vreven, J. A. Montgomery, Jr., J. E. Peralta, F. Ogliaro, M. Bearpark, J. J. Heyd, E. Brothers, K. N. Kudin, V. N. Staroverov, R. Kobayashi, J. Normand, K. Raghavachari, A. Rendell, J. C. Burant, S. S. Iyengar, J. Tomasi, M. Cossi, N. Rega, J. M. Millam, M. Klene, J. E. Knox, J. B. Cross, V. Bakken, C. Adamo, J. Jaramillo, R. Gomperts, R. E. Stratmann, O. Yazyev, A. J. Austin, R. Cammi, C. Pomelli, J. W. Ochterski, R. L. Martin, K. Morokuma, V. G. Zakrzewski, G. A. Voth, P. Salvador, J. J. Dannenberg, S. Dapprich, A. D. Daniels, Ö. Farkas, J. B. Foresman, J. V. Ortiz, J. Cioslowski, and D. J. Fox, Gaussian, Inc., Wallingford CT, 2009.
[S13] (a) Reed, A. E.; Weinhold, F. *J. Chem. Phys*. **1983**, *78*, 4066. (b) Reed, A. E.; Weinstock, R. B.; Weinhold, F. *J. Chem. Phys*. **1985**, *83*, 735. (c) Reed, A. E.; Curtiss, L. A.; Weinhold, F. *Chem. Rev.*, **1988**, *88*, 899.
[S14] Wiberg, K. *Tetrahedron*, **1968**, *24*, 1083.
[S15] NBO Version 3.1, Glendening, E. D.; Reed, A. E.; Carpenter J. E. and Weinhold, F.
[S16] Gabedit is a free Graphical User Interface for computational chemistry packages. It is written by Abdul-Rahman Allouche. Gabedit is available from http://lasim.univ-lyon1.fr/allouche/gabeditb.
[S17] Schaftenaar, G.; Noordik, J.H. *J. Comput.-Aided Mol. Design*, **2000**, *14*, 123.
